Supporting Information

Hierarchically self-assembled MOF network enables continuous ion transport and high mechanical strength

Lulu Du, Bo Zhang, Wei Deng, Yu Cheng, Lin Xu, and Liqiang Mai**

L.L. Du, W. Deng, Y. Cheng, Prof. L. Xu, Prof. L.Q. Mai
State Key Laboratory of Advanced Technology for Materials Synthesis and Processing,
School of Materials Science and Engineering, Wuhan University of Technology,
Luoshi Road 122, Wuhan, 430070, P. R. China.
E-mail: linxu@whut.edu.cn; mlq518@whut.edu.cn

Prof. L. Xu, Prof. L.Q. Mai
Foshan Xianhu Laboratory of the Advanced Energy Science and Technology Guangdong Laboratory, Foshan 528200, China.
E-mail: linxu@whut.edu.cn; mlq518@whut.edu.cn

B. Zhang
State Key Laboratory of Advanced Technology for Materials Synthesis and Processing
International School of Materials Science and Engineering
Wuhan University of Technology
Wuhan 430070, China

Experiment

Materials: The following chemicals were used as received without further purification: KOH (99%, Aladdin), $Zn(NO_3)_2·6H_2O$ (99%, Aladdin), 2-methylimidazole (2-MIM, 98%, Aladdin), 1-Ethyl-3-methylimidazolium bis(trifluoromethylsulfonyl)imide (EMIM-TFSI, 99%, Aladdin) and Bis(trifluoromethane)sulfonimide lithium salt (LiTFSI, 99%, Aladdin), N, N-dimethyl formamide (DMF, 99%, Aladdin), poly(vinylidene fluoride) (PVDF, Arkema, Kynar 761).

Fabrication of hierarchically self-assembled MOF network: The porous polyimide film was purchased from Jiangxi Advanced Nanofiber S&T Co. Ltd, which was treated with ultrasonication to remove impurities for 10 min and washed three times using ethanol, and finally dried at 80 ℃ for 12 h. Surface alkaline etching was then performed on the polyimide film by immersing in a 1 M KOH solution for 30 min and then washed thoroughly by deionized water to remove the remnant KOH. The etched polyimide network was then immersed into the solution containing 3g Zn $(NO_3)_2·6H_2O$ and 70 ml methanol for 30 min. then a solution containing 6.5 g 2-MIM and 70 ml methanol was added into above mixture with stirring for 15 h. Finally, the hierarchically self-assembled MOF network was obtained after thermal treatment in nitrogen atmosphere to 280 °C for 2 h.

Fabrication of conventional MOF powders: Conventional MOF powder was synthesized for fair comparison at room temperature. In a typical process, 3 g Zn $(NO_3)_2·6H_2O$ and 6.5 g 2-MIM were dissolved in 70 mL methanol, respectively. Afterwards, the 2-MIM methanolic solution was added into Zn $(NO_3)_2·6H_2O$ methanolic solution stirring for 15 h at room temperature. Finally, the product was collected by centrifugation and washed with methanol, and then dried at 80 °C.

Fabrication of hierarchically self-assembled MOF network ionic conductor: LiTFSI (0.26 g) was dissolved in EMIM-TFSI (1 mL) by magnetic stirring at room temperature for 1h. The resultant solution was heated at 120 ℃ for overnight to obtain lithium ionic liquid (Li-IL). Afterwards, the hierarchically self-assembled MOF network was soaked in above lithium ionic liquid and heated at 100 ℃ in the vacuum overnight. The resulting 3D ionic conductor can be obtained by vacuum filtration to remove the excessive ionic liquid.

Fabrication of MOF network-PVDF composite solid electrolyte: PVDF powder was dried under vacuum at 100 °C overnight to remove moisture. Polymer electrolyte solution was prepared by dissolving PVDF and LiTFSI at a weight ratio of 6:5 in DMF with a polymer concentration of 10 wt% and the mixed suspension was magnetically stirred at 60 °C for 24 h

to obtain homogeneous solution. Then the self-assembled MOF network ionic conductor was wet by the PVDF-based gel and dried at 80 °C in the vacuum oven for 24 h. This wetting-then-drying process was repeated several times until the self-assembled MOF network ionic conductor was fully embedded in PVDF matrix. In addition, PVDF/LiTFSI polymer electrolytes and PVDF/LiTFSI polymer electrolytes with randomly distributed MOF powder with IL as fillers were prepared via a typical casting-then-drying approach as control samples.

Preparation of cathode and cell assembly: Commercial $LiFePO_4$, super-P, PVDF and LiTFSI were mixed in N-methyl pyrrolidone (NMP) with a mass ratio of 8:1:0.5:0.5 to obtain the cathode mixture. And the cathode mixture was subsequently coated on Al foil. The prepared electrode films were dried at 120 ℃ for 24 h under vacuum before cell fabrication, and the mass loading was ~2 mg/cm^2. Finally, different solid electrolytes were sandwiched between $LiFePO_4$ and Li foil with a thickness of 500 μm for coin cell assembly to study their electrochemical performance. In aiidtion, $LiNi_{0.8}Co_{0.1}Mn_{0.1}O_2$ (NCM811) was used as the high-voltage cathode material. NCM811, Super P, PVDF and LiTFSI were mixed evenly in NMP with a mass ratio of 8:1:0.5:0.5 to form a uniform slurry, followed by coating on Al foil. Then the mixture was dried at 120 ℃ in vacuum for 12 h, and the mass loading was ~2 mg/cm^2. The battery performance of Li-NCM811 cell using Li foil with a thickness of 500 μm was tested at room temperature. In order to investigate the potential for practical application, we assembled the pouch cells using $LiFePO_4$ cathode with mass loading 25 mg cm^{-2} (70 cm^{-2}), and limited Li metal anode a thickness of 100 μm (70 cm^{-2}). Based on this, the N/P ratio of the pouch cells in this work was 5. In order to improve the poor solid-solid contact between solid electrolytes and electrodes, little ionic liquid (~3 μL/cm^2) is added to the interface between obtained solid electrolytes and cathode to reduce the interface resistance.

Materials Characterization: The overall morphology and nanostructure were investigated by Field Emission Scanning Electron Microscope (FSEM JEOL JSM-7100FA) with an acceleration voltage of 20kV. Elemental analysis was performed by the Energy Dispersive X-ray spectroscope (Oxford IE250 system). TEM images were captured and recorded by using JEM-2100F with acceleration voltage 200kV. Crystallographic characterization was conducted by D8 Discover X-ray diffractometer using Cu-Kα X-ray source with radiation (λ = 1.5418 Å). FT-IR measurements were obtained using Nicolet 6700 (Thermo Fisher Scientific Co., USA) IR spectrometer with a wavenumber range from 400 to 4000 cm^{-1}. Thermogravimetric analysis (TGA) was performed in the air atmosphere from 30 to 800 °C with a heating rate of 10 °C min^{-1} using Netzsch STA 449C simultaneous analyzer. The N_2

adsorption/desorption isothermal was performed by the TriStar-3020 gas adsorption analyzer at 77 K (Micromeritics Instrument Co., USA). The X-ray photoelectron spectroscopy (XPS) analysis was carried out by ESCALAB 250 Xi spectrometer (VG Scientific Co., UK). Stress-Strain curves were tested by Instron 5967.

Electrochemical Measurements: Ionic conductivity was determined by EIS after placing the solid electrolyte between two electrodes (stainless steel) contacts in a CR2016 coin cell. Autolab PGSTAT302N was used for measurements at various temperatures from 20 to 80 °C with a step size of 10 °C and frequency ranges from 10^6 to 0.1 Hz. The bulk resistance of the samples was calculated from the EIS curve. The ionic conductivity was obtained using equation (1):

$$\sigma = \frac{d}{SR_b} \quad (1)$$

where S and d represent the area and thickness of the solid electrolyte pellets, respectively. R_b is the bulk resistance, and σ is the ionic conductivity (S cm^{-1}).

The activation energy Ea was calculated according to Arrhenius equation (2):

$$\sigma = AT^{-1}e^{-E_a/RT}$$

The value of prefactor A is related to the effective charge carrier concentration.

The electrochemical stability window was tested by linear sweep voltammetry (LSV) on a lithium|solid electrolyte|stainless steel cell from 0 to 6.5 V via Autolab PGSTAT302N at a scan rate of 10 mV s^{-1}.

The Li-ion transference number (t_{Li^+}) was tested in symmetric lithium cell using a Autolab PGSTAT302N at room temperature by a combination of DC polarization and AC impedance measurement. A DC potential (ΔV=10 mV) was applied for 5500 s to gain the initial and steady currents. Meanwhile, the AC impedance spectra of the same cell were measured before and after polarization. The value of lithium transference number (t_{Li^+}) have been calculated by equation (3):

$$t_{Li^+} = \frac{I_s(\Delta V - I_0R_0)}{I_0(\Delta V - I_sR_s)}$$

Where R_0 and R_s are the AC impedances before and after polarization, respectively. I_0 and I_s are the initial and steady currents respectively.

Cycling stability of solid electrolytes against lithium metals was measured by Li symmetrical cell using a LANHE CT2001A charge/discharge system at different current densities at room temperature with 2 h charge/discharge cycles.

The cycle performance and specific capacity of different solid electrolytes were measured by full cells ($LiFePO_4$//Li) using a LANHE CT2001A charge/discharge system.

Results and Discussion

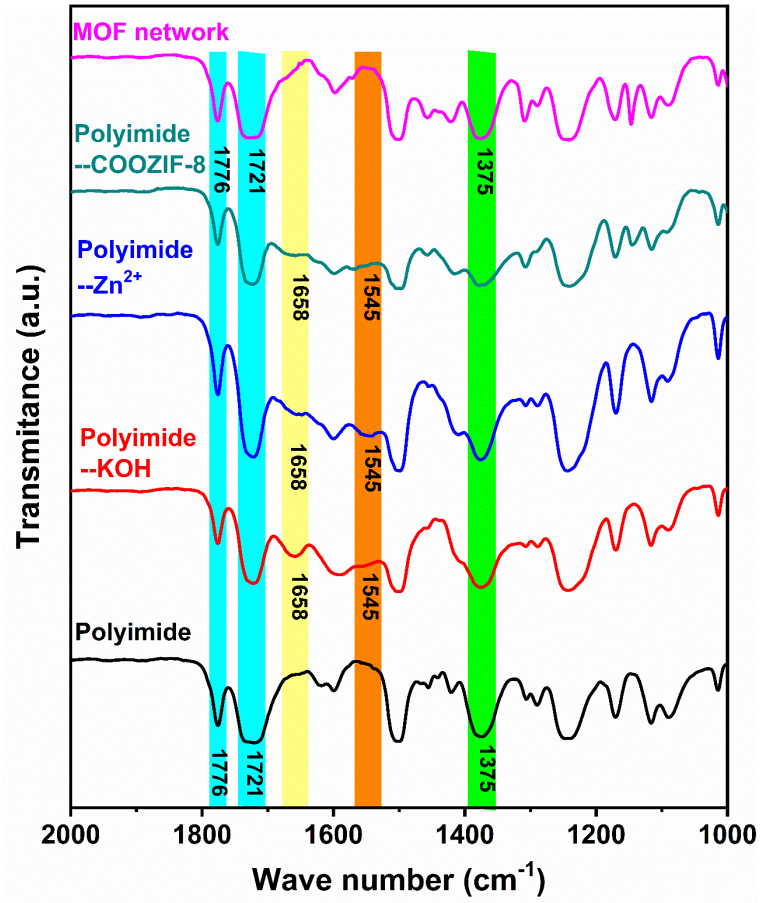

Figure S1. FTIR spectra of polyimide, polyimide after KOH treatment, polyimide after Zn^{2+} exchange and MOF network before after thermal treatment.

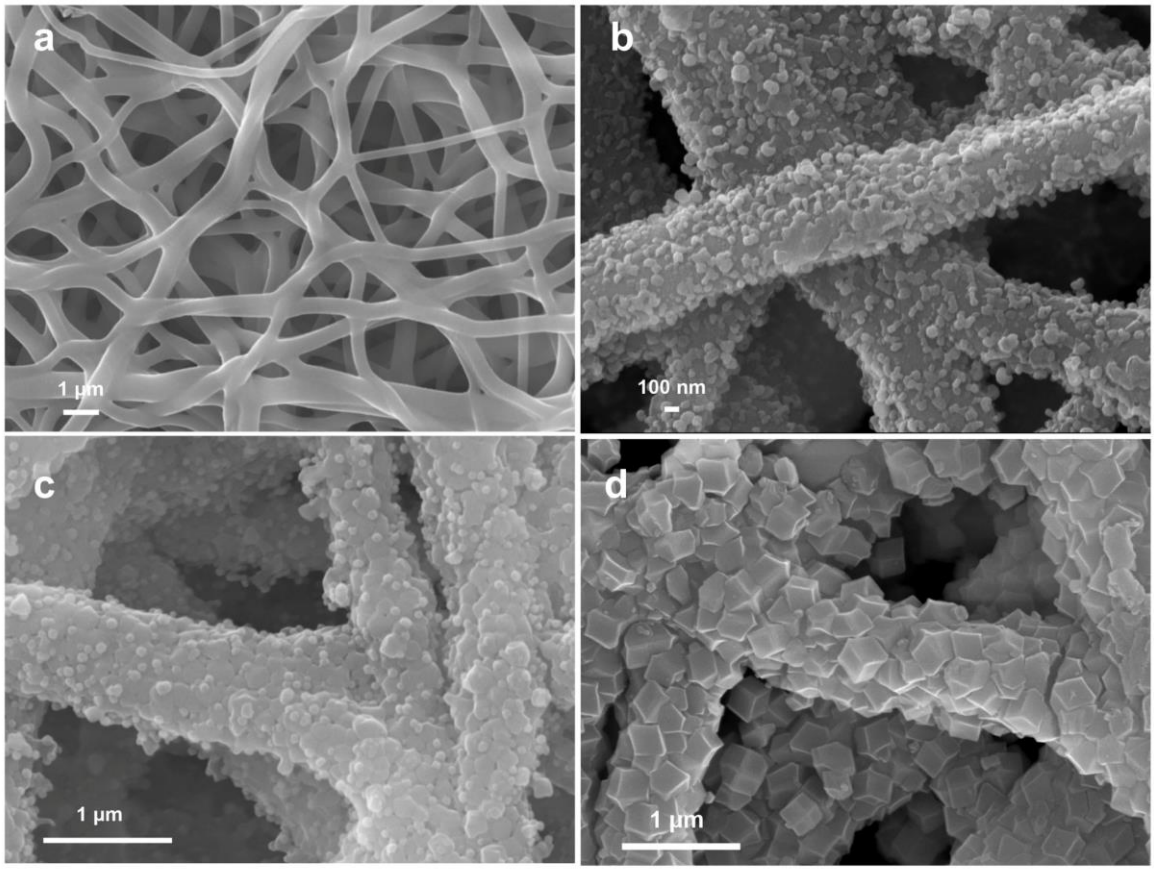

Figure S2. SEM images of self-assembled MOF network with different reaction times. (a) 0 h. (b) 5 h. (c) 10 h. (d) 15 h.

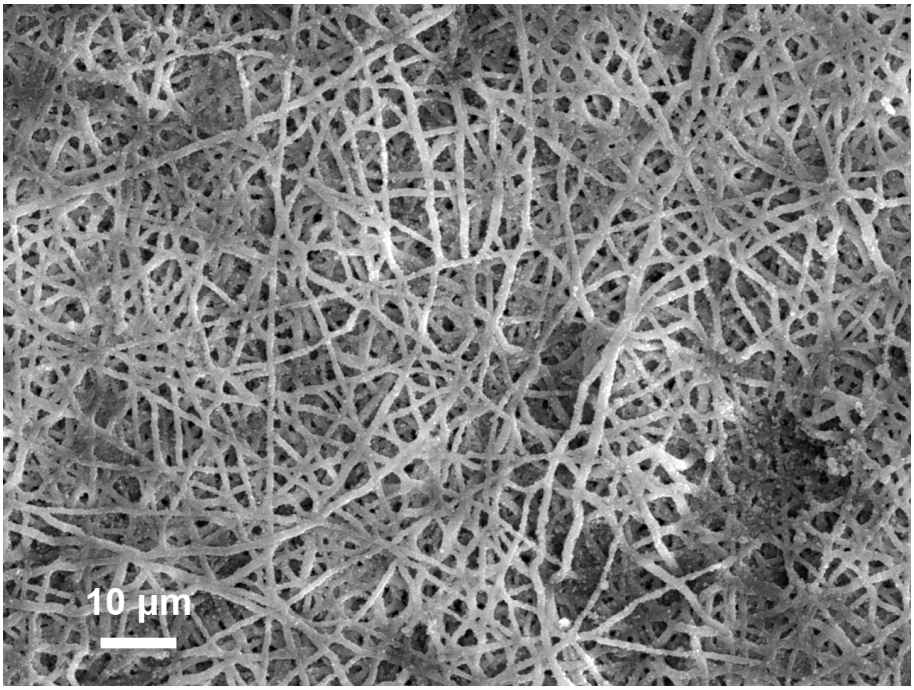

Figure S3. SEM images of the hierarchically self-assembled MOF network.

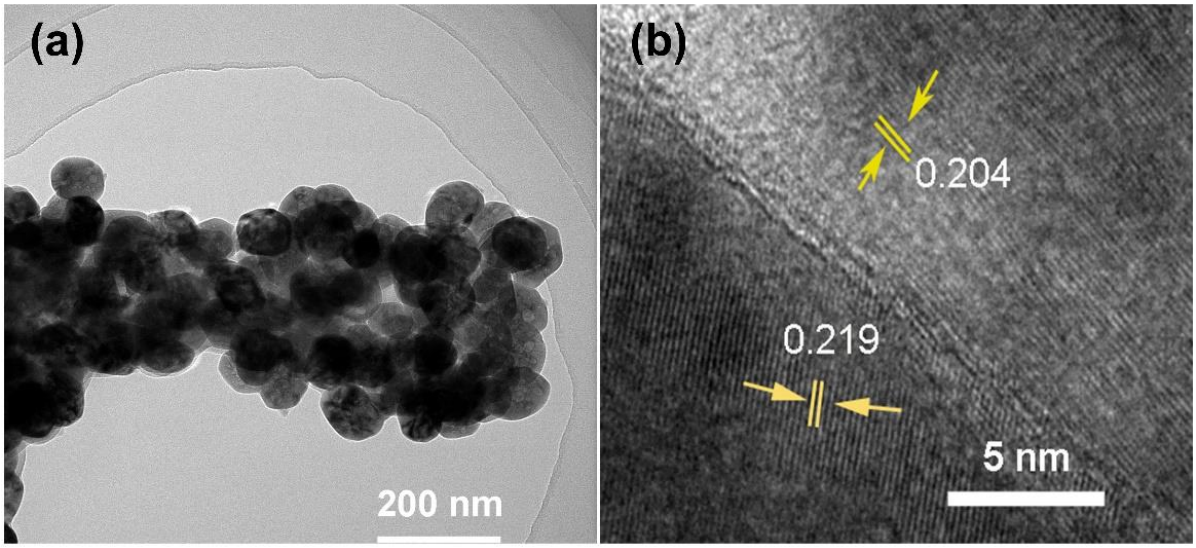

Figure S4. TEM images of the hierarchically self-assembled MOF network with different magnifications.

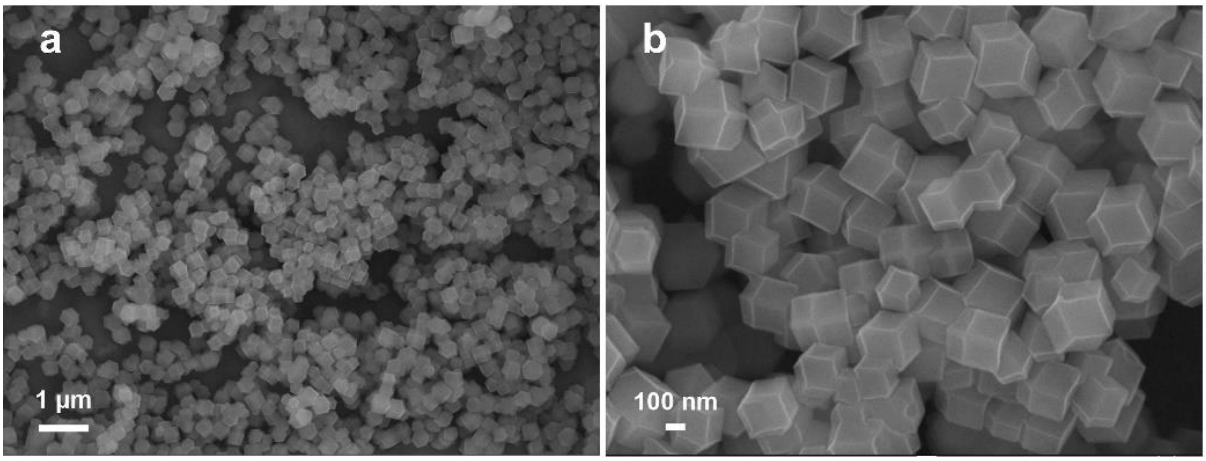

Figure S5. SEM images of typical MOF powder.

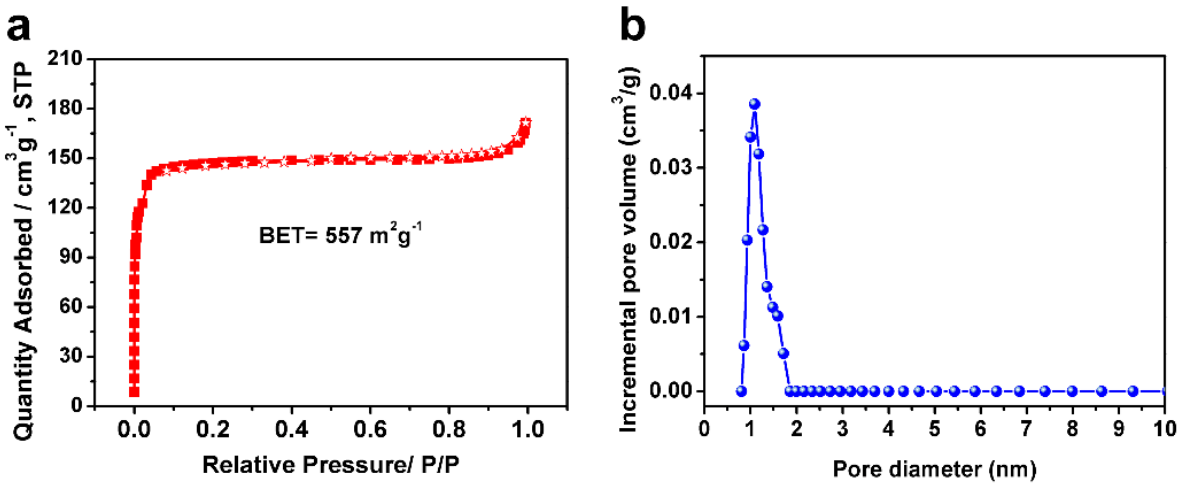

Figure S6. (a) N_2 adsorption-desorption isotherms and (b) Related pore size distribution of the hierarchically self-assembled MOF network, respectively.

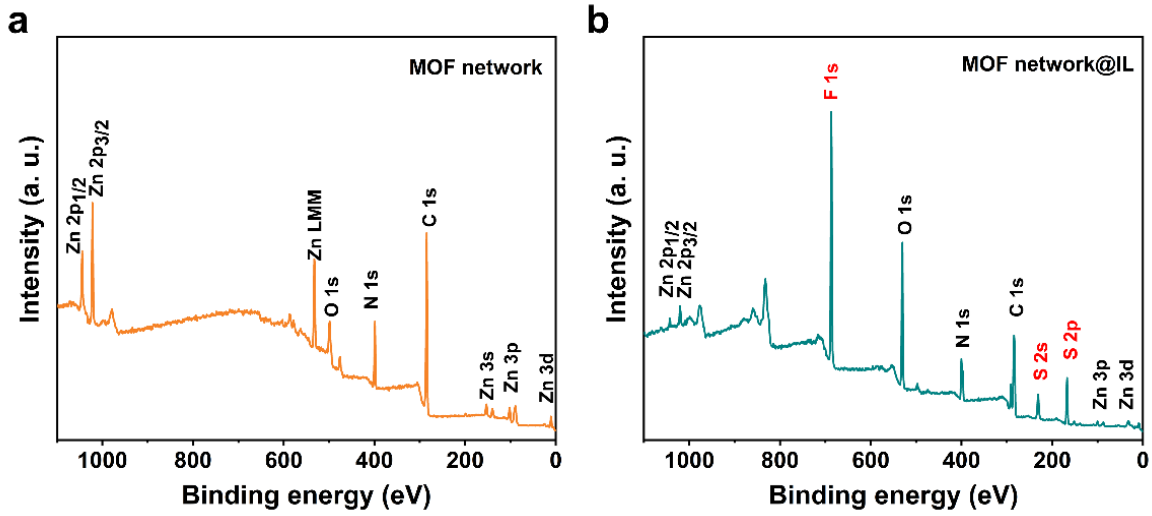

Figure S7. XPS survey spectrum of (a) Pristine hierarchically self-assembled MOF network. (b) Hierarchically self-assembled MOF network impregnated with ionic liquid.

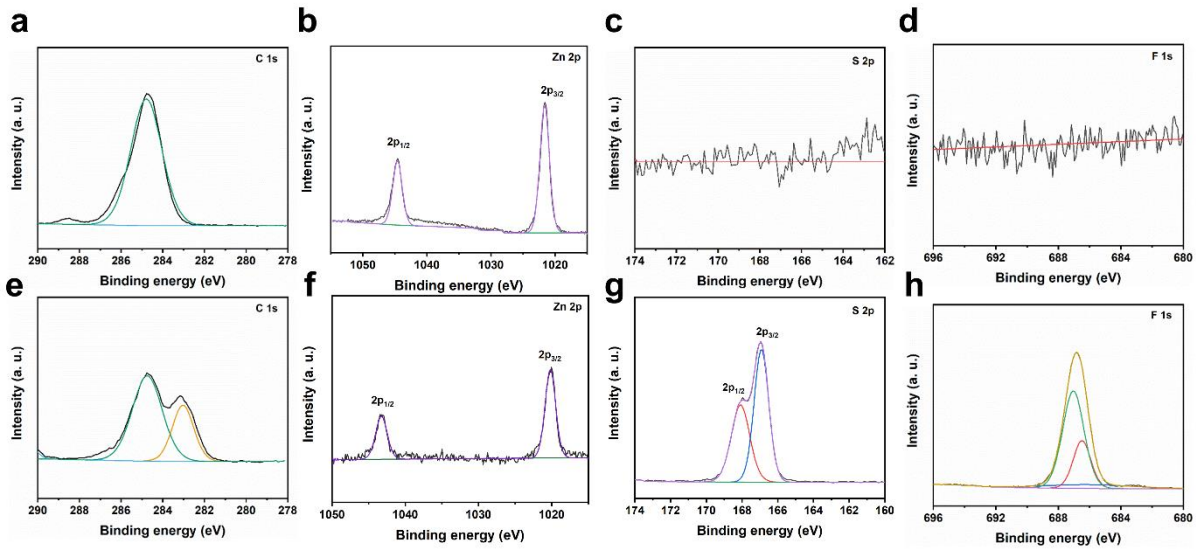

Figure S8. XPS spectra (a-d) Pristine hierarchically self-assembled MOF network. (e-h) Hierarchically self-assembled MOF network impregnated with ionic liquid.

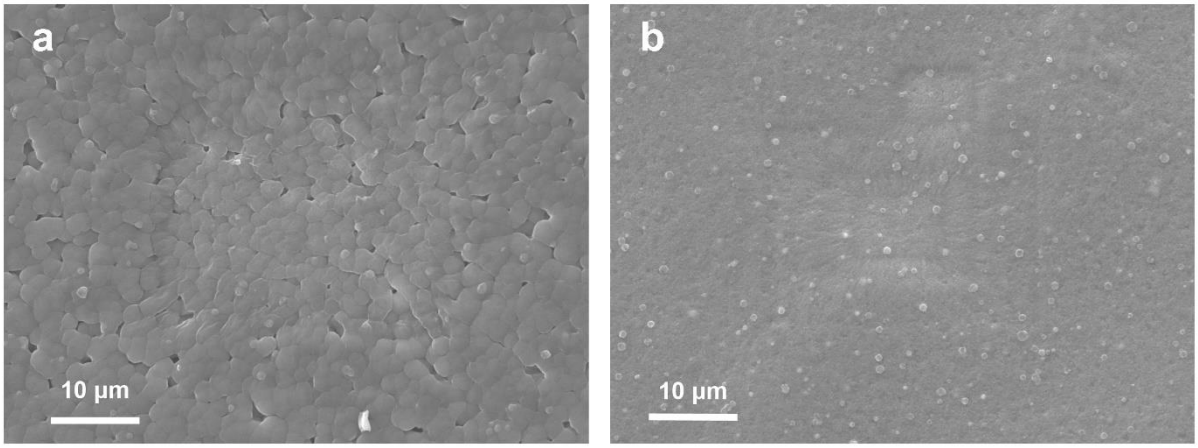

Figure S9. SEM images of (a) Pure PVDF solid electrolyte. (b) MOF powder-PVDF composite solid electrolyte .

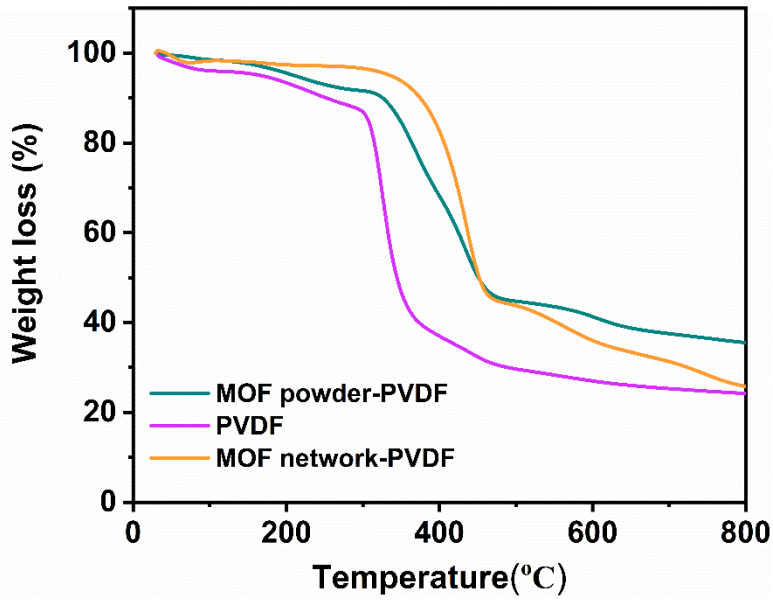

Figure S10. TG curves of different solid electrolytes.

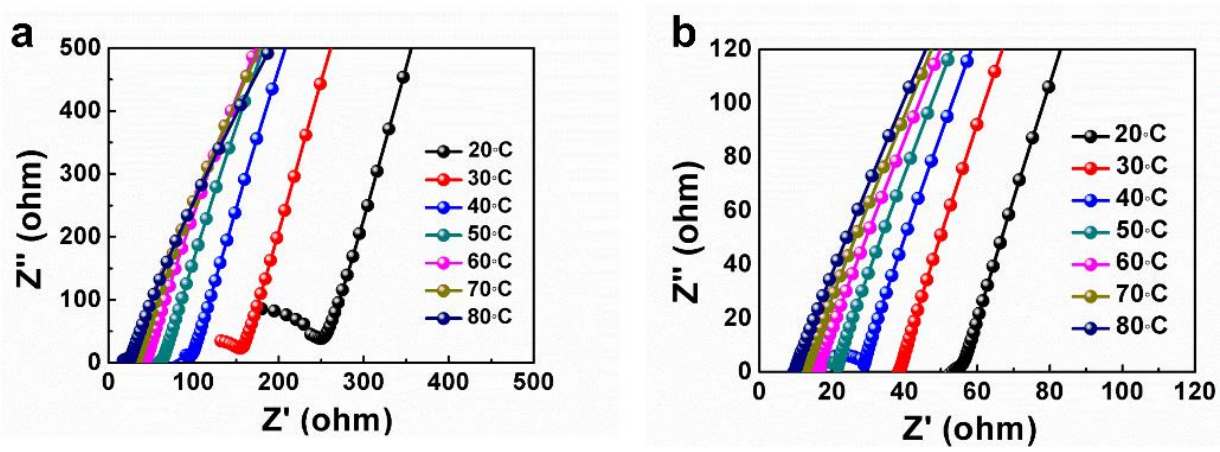

Figure S11. Typical EIS plots at different temperatures. (a) Pure PVDF solid electrolyte. (b) MOF powder-PVDF composite solid electrolyte.

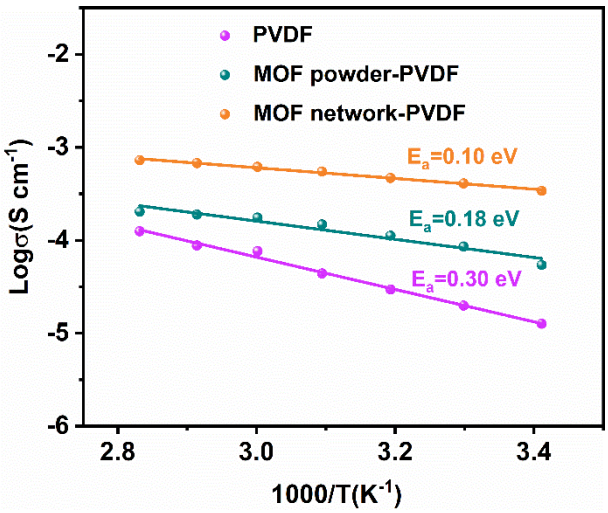

Figure S12. Arrhenius plots of PVDF, MOF powder-PVDF and MOF network-PVDF solid electrolytes.

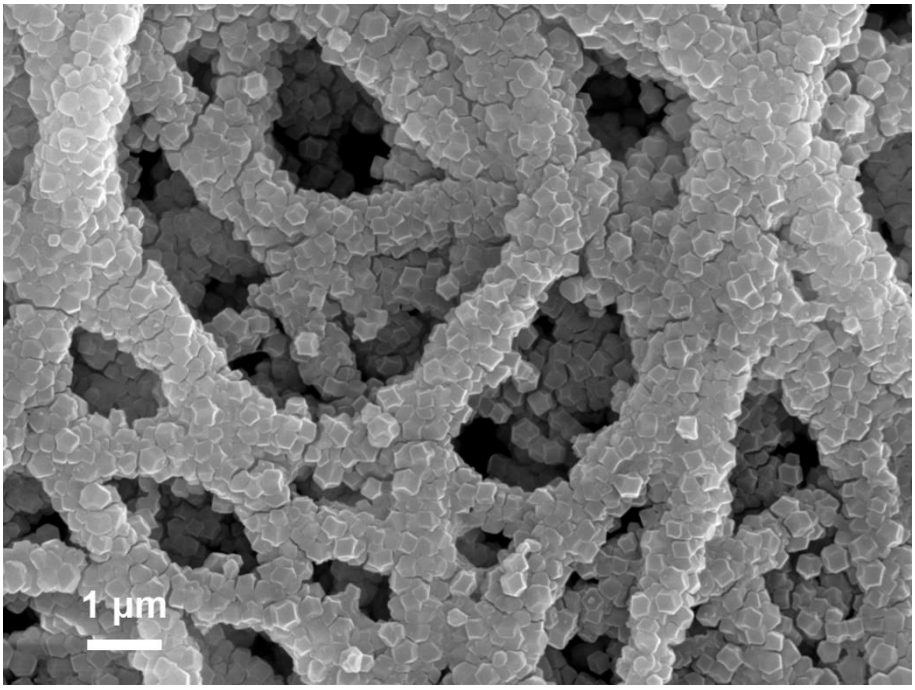

Figure S13. SEM images of the hierarchically self-assembled MOF network after vigorous stirring (600 rpm) in methanol for 48 h.

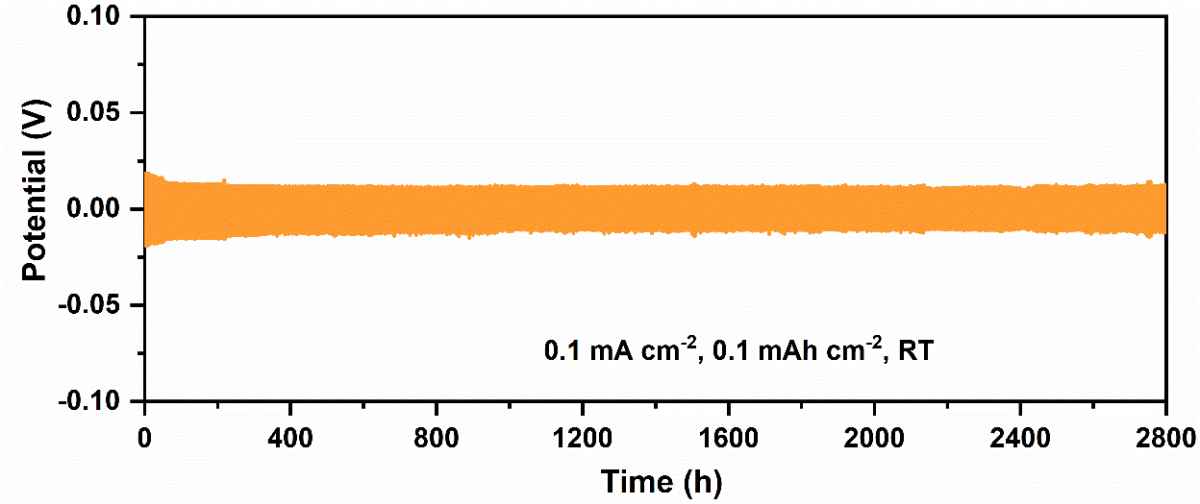

Figure S14. Cycling performance of Li symmetric cells with hierarchically self-assembled MOF network based solid electrolyte at current densities of 0.1 mA cm^{-2} at room temperature

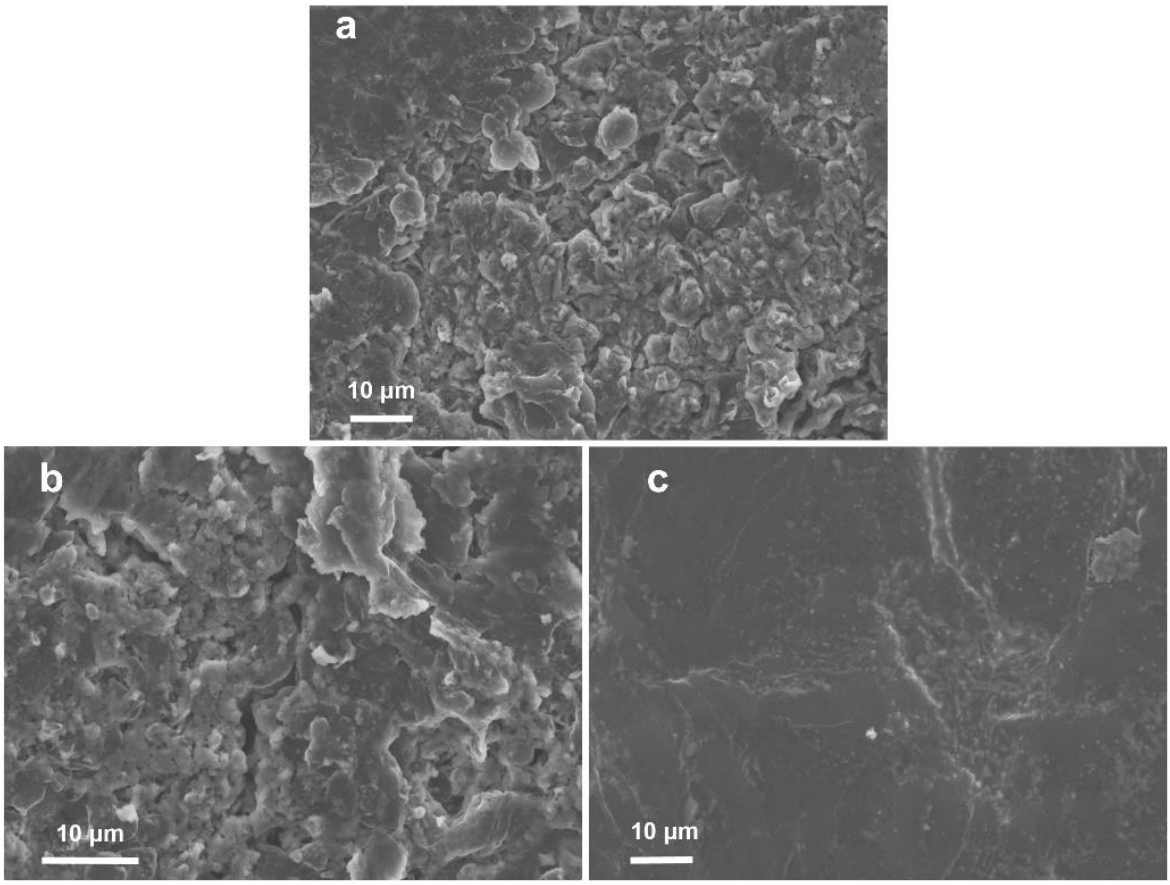

Figure S15. SEM images of Li metal after long-term cycle in Li/Li cells at 0.4 mA cm^{-2} (a) Pure PVDF solid electrolyte. (b) MOF powder-PVDF composite solid electrolyte. (c) MOF network-PVDF composite solid electrolyte.

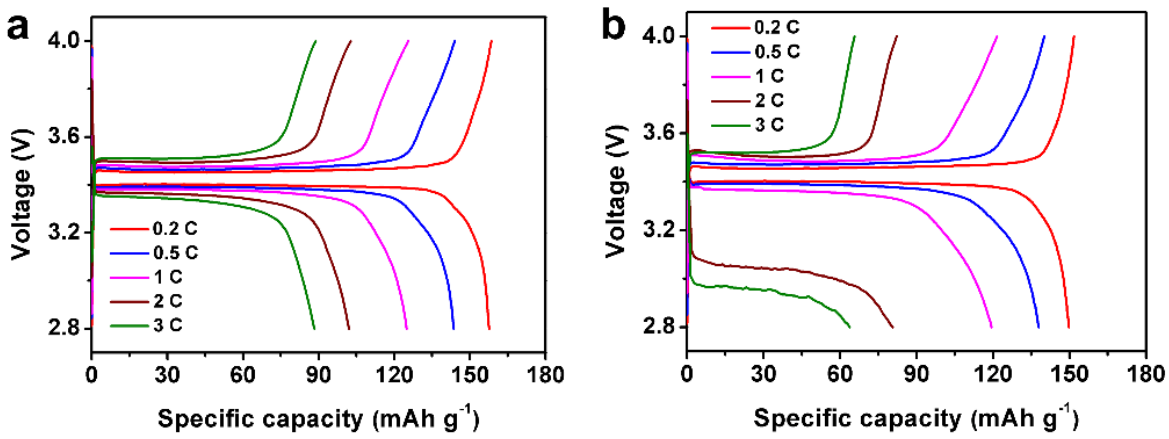

Figure S16. Charge and discharge voltage profiles of $LiFePO_4$/Li batteries at different rates using different solid electrolytes. (a) MOF powder-PVDF composite solid electrolyte. (b) Pure PVDF composite solid electrolyte.

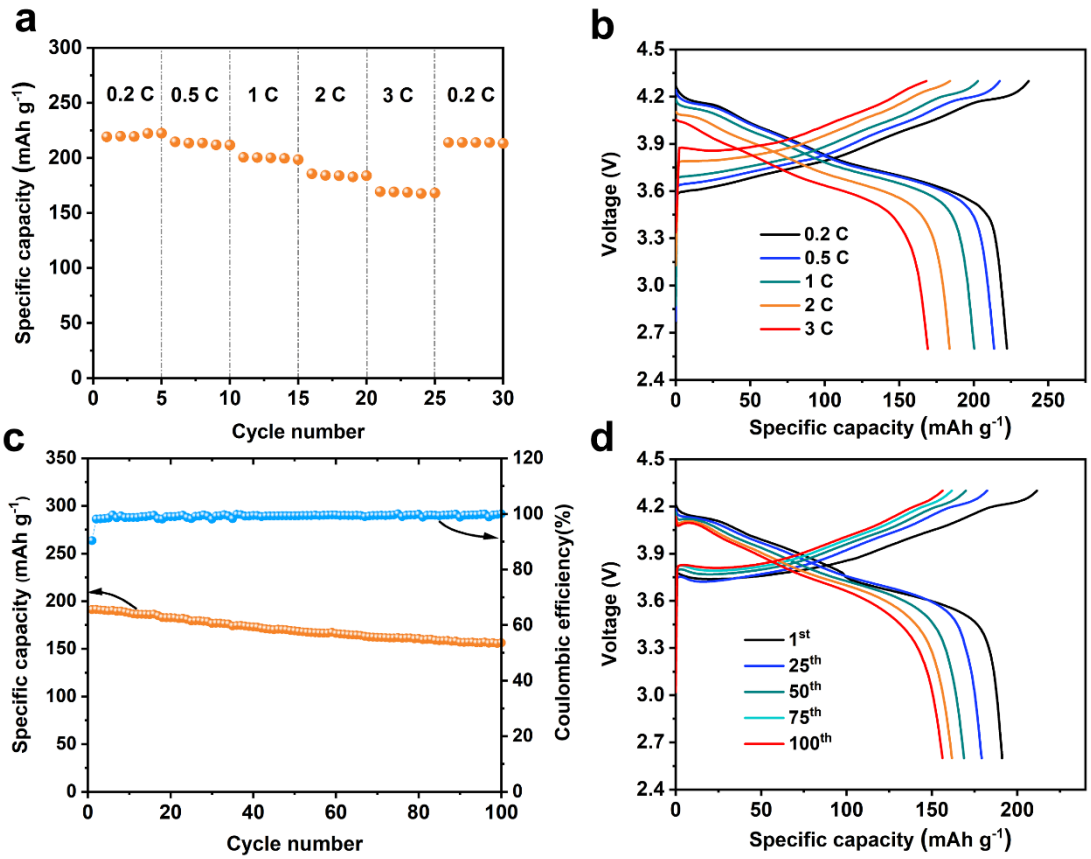

Figure S17. Electrochemical performance of NCM811//Li batteries using the MOF network-PVDF composite solid electrolyte at room temperature. (a) Rate performance at current rates of 0.2, 0.5, 1, 2, and 3 C, respectively. (b) Voltage curves at current rates of 0.2, 0.5, 1, 2, and 3 C, respectively. (c) Cycling performances at 1 C. (d) Charge and discharge voltage profiles at different cycling numbers.